Numerical Analysis of Nanotube Based NEMS Devices — Part II: Role of Finite Kinematics, Stretching and Charge Concentrations

Changhong Ke

Horacio D. Espinosa[1]
e-mail: espinosa@northwestern.edu

Nicola Pugno[2]

Department of Mechanical Engineering,
Northwestern University,
Evanston, IL 60208-3111

In this paper a nonlinear analysis of nanotube based nano-electromechanical systems is reported. Assuming continuum mechanics, the complete nonlinear equation of the elastic line of the nanotube is derived and then numerically solved. In particular, we study singly and doubly clamped nanotubes under electrostatic actuation. The analysis emphasizes the importance of nonlinear kinematics effects in the prediction of the pull-in voltage of the device, a key design parameter. Moreover, the nonlinear behavior associated with finite kinematics (i.e., large deformations), neglected in previous studies, as well as charge concentrations at the tip of singly clamped nanotubes, are investigated in detail. We show that nonlinear kinematics results in an important increase in the pull-in voltage of doubly clamped nanotube devices, but that it is negligible in the case of singly clamped devices. Likewise, we demonstrate that charge concentration at the tip of singly clamped devices results in a significant reduction in pull-in voltage. By comparing numerical results to analytical predictions, closed form formulas are verified. These formulas provide a guide on the effect of the various geometrical variables and insight into the design of novel devices. [DOI: 10.1115/1.1985435]

1 Introduction

Nano-electromechanical systems (NEMS) are attracting significant attention because of their properties to enable superior electronic computing and sensing. By exploiting nanoscale effects, NEMS present interesting and unique characteristics. For instance, NEMS based devices can have an extremely high fundamental mechanical oscillation frequency [1–4], while preserving a robust mechanical response [5]. Several NEMS applications have been proposed, such as mass sensors [6], rf resonators [6], field effect transistors [7] and electrometers [8]. Carbon nanotubes (CNTs) have long been considered ideal building blocks for NEMS devices due to their superior electromechanical properties. CNT-based NEMS reported in the literature include nanotweezers [9,10], nonvolatile random access memory devices [11], nanorelays [12], rotational actuators [13] and recently proposed feedback-controlled nanocantilever NEMS devices [14]. All these reported devices can be simply modeled as CNT cantilevers or fixed-fixed CNTs hanging over an infinite conductive substrate. In order to design a functional NEMS device, its electromechanical characteristic should be well quantified in advance. During the past years, a lot of progress has been achieved in regard to the modeling of CNT-based nano-devices [15]. Generally, sufficiently large diameter multiwalled carbon nanotubes (MWNTs), i.e., with

diameters of ~20 nm and higher, can be modeled to a good approximation as homogeneous cylindrical beams and perfect conductors, meaning that quantum effects and finite scale charge distribution are negligible at this dimension [16]. Three main types of forces have to be considered in the modeling of the electromechanical characteristic of CNT-based NEMS devices: the elastic forces, the electrostatic forces, and the van der Waals forces arising from the atomic interactions. For the elastic restoring forces, the classical continuum mechanics theory is applicable to CNT devices as demonstrated by molecular dynamics simulation [15]. The electrostatic forces are typically computed by using a capacitance model [17], so that a precise modeling of the capacitance of CNTs is a key issue in their description. We discuss this point, emphasizing the role of charge concentration at the tip of cantilever nanotubes, based on classical electrostatics. For the van der Waals forces, a continuum model based on Lennard-Jones potential theory was employed in the literature [15]. The effect of the van der Waals force on the performance of the CNT devices could be significant in the case of small gaps between nanotube and substrate or for sufficiently long nanotubes [14,15]. Another important but typically omitted effect in the modeling of nanodevices is finite kinematics, which accounts for large displacements. Note that for doubly clamped nanotubes, a dramatic increase in the elastic energy stored in the nanotube is expected as a consequence of the stretching imposed by the rope-like behavior. In this paper, we investigate the electromechanical characteristics of singly and doubly clamped CNT-based NEMS, as illustrated in Fig. 1: a biased MWNT cylinder of length L, placed above an infinite ground plane, at a height H. The inner radius and outer radius of MWNT are R_{int} and R_{ext}, respectively. The applied voltage between nanotube and substrate is V.

The paper is organized as follows. First, an analysis of the charge distribution arising from the electrostatic field is presented. The nonlinear elastic line equation is then derived. This equation is integrated numerically and compared to analytical predictions

Fig. 1 Schematic of nanotube based NEMS devices

Fig. 3 Schematic of the finite kinematics configuration of a cantilever nanotube device subjected to electrostatic forces and van der Waals forces

derived elsewhere. We close the paper with conclusions concerning the conditions under which finite kinematics and end charge concentration cannot be neglected for two boundary conditions, singly and doubly clamped devices.

2 Analysis of Charge Distribution

During the past years, significant progress has been made in regard to the computation of the charge distribution along finite-length nanotubes. For conductive nanotubes, essentially classical distribution of charge density with a significant charge concentration at the tube end has been observed [18–20]. Recently a model based on three-dimensional electrostatic calculations has been proposed in [21] to describe the charge distribution along finite length MWNTs cylinder, in particular, the concentrated charges at the tube ends.

Figure 2 shows the charge distribution along the length of a freestanding nanotube of length L, subjected to a bias voltage of 1 V. The contour plot shows the charge density (side view), while the curve shows the charge per unit length along the nanotube. The calculation is performed using the CFD-ACE+ software (a commercial code from CFD Research Corporation based on finite and boundary element methods). The calculations and model reported in [21] are valid as long as the conductive nanotube radius, R_{ext}, is larger than ~10 nm, and the length of the tube, L, is much larger than H and R_{ext}. In these cases quantum effects and size-limit effects in the charge distribution can be considered negligible [21].

The capacitance per unit length along the cantilever nanotube, under moderate deflections, is approximated as [21]

$$C[r(x)] = C_d[r(x)]\{1 + 0.85[(H + R_{\text{ext}})^2 R_{\text{ext}}]^{1/3}\delta(x - x_{\text{tip}})\}$$
$$= C_d[r(x)]\{1 + f_c\}, \quad (1)$$

where the first term in the bracket accounts for the uniform charge along the side surface of the tube and the second term, f_c, accounts for the concentrated charge at the end of the tube; $x=x_{\text{tip}} \neq L$, as a result of the finite kinematics; $\delta(x)$ is the Dirac distribution function. $C_d[r(x)]$ is the distributed capacitance along the side surface per unit length for an infinitely long tube, which is given by [17]
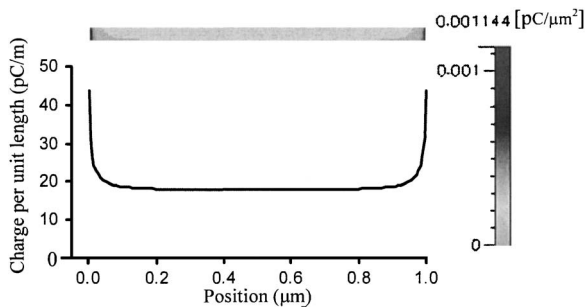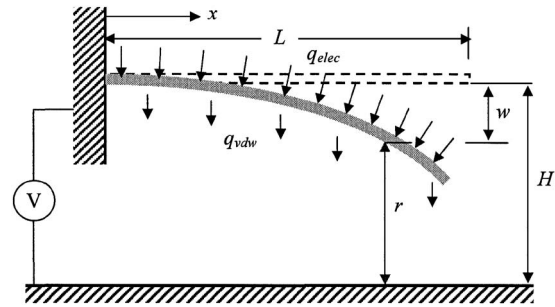

Fig. 2 Charge distribution for a biased nanotube. The device parameters are $R_{\text{ext}}=9$ nm, $H=100$ nm and $L=1$ μm.

$$C_d[r(x)] = \frac{2\pi\varepsilon_0}{a\cosh\left(1 + \dfrac{r(x)}{R_{\text{ext}}}\right)} \quad (2)$$

where r is the distance between the lower fiber of the nanotube and the substrate, and ε_0 is the permittivity of vacuum ($\varepsilon_0 = 8.854 \times 10^{-12}$ C^{2}N^{-1} m^{-2}). Thus, the electrostatic force per unit length of the nanotube is given by differentiation of the energy as follows:

$$q_{\text{elec}} = \frac{1}{2}V^2\frac{dC}{dr} = \frac{1}{2}V^2\left(\frac{dC_d}{dr}\right)\{1 + f_c\}$$
$$= \frac{\pi\varepsilon_0 V^2}{\sqrt{r(r + 2R_{\text{ext}})}\,a\cosh^2\left(1 + \dfrac{r}{R_{\text{ext}}}\right)}(1 + f_c) \quad (3)$$

In the above equation $r(x)=H-w(x)$, with w being the deflection and V the bias voltage.

3 Nonlinear Elastic Line Equations

3.1 Singly Clamped Nanotube. The deflection of a cantilver nanotube under electrostatic force and van der Waals force is shown in Fig. 3. The electrostatic force per unit area remains perpendicular to the outer surface of the nanotube under finite kinematics as imposed by the electrical field. The electrostatic force per unit length of the cylinder is also perpendicular to the cylinder axis. Here we ignore the force applied to the end surface of the cantilever.

Accordingly, if we just consider the bending of the cantilever, the governing equation of the elastic line under finite kinematics is [22]

$$EI\frac{d^2}{dx^2}\left(\frac{\dfrac{d^2w}{dx^2}}{\left(1 + \left(\dfrac{dw}{dx}\right)^2\right)^{3/2}}\right) = (q_{\text{vdw}} + q_{\text{elec}})\sqrt{1 + \left(\frac{dw}{dx}\right)^2}, \quad (4)$$

where E is the Young modulus, $I=\pi(R_{\text{ext}}^4 - R_{\text{int}}^4)/4$ is the moment of the inertia of the nanotube; q_{vdw} is the van der Waals force (per unit length) between the nanotube and the substrate and can be evaluated by the method reported in [15], assuming the substrate consists of 30 graphite layers. Equation (4) represents the elastic line equations for a nanotube under finite kinematics. As a consequence of the large flexibility of the nanotube, it remains in the elastic regime. Equation (4) clearly represents a more accurate description of the elastic behavior of nanotubes, than the more common equation assuming small displacements, i.e., $dw/dx \ll 1$

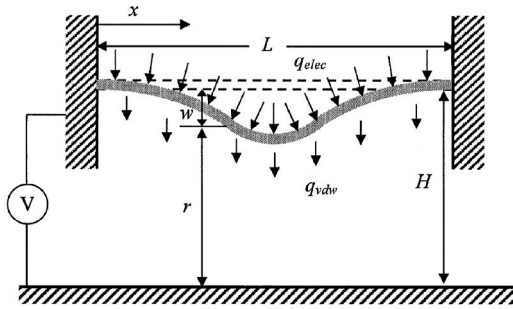$$EI\frac{d^4w}{dx^4} = q_{\text{elec}} + q_{\text{vdw}} \quad (5)$$

Fig. 4 Schematic of the finite kinematics configuration of a fixed-fixed nanotube device subjected to electrostatic forces and van der Waals forces

Fig. 6 Electromechanical characteristic (central displacement-voltage curve) for fixed-fixed nanotube device. The dashed line is for small deformation model (pure bending), the solid line is for finite kinematics model (bending plus stretching).

3.2 Doubly Clamped Nanotube. For a doubly clamped nanotube, stretching becomes significant as a consequence of the rope-like behavior of a fixed-fixed nanotube subjected to finite kinematics shown in Fig. 4. A tension T in the nanotube has to be introduced, so that the elastic line equation becomes [22]

$$EI\frac{d^2}{dx^2}\left(\frac{\frac{d^2w}{dx^2}}{\left(1+\left(\frac{dw}{dx}\right)^2\right)^{3/2}}\right) - T\left(\frac{\frac{d^2w}{dx^2}}{\left(1+\left(\frac{dw}{dx}\right)^2\right)^{3/2}}\right)$$
$$= (q_{vdw} + q_{elec})\sqrt{1+\left(\frac{dw}{dx}\right)^2} \qquad (6)$$

The tension T is related to the axial strain ε, namely [23],

$$T = EA\varepsilon \approx \frac{EA}{2L}\int_0^L\left(\frac{dw}{dx}\right)^2 dx \qquad (7)$$

where A is the cross-sectional area of the nanotube. Combining Eqs. (6) and (7), we can obtain the governing elastic line equation for the equilibrium position as
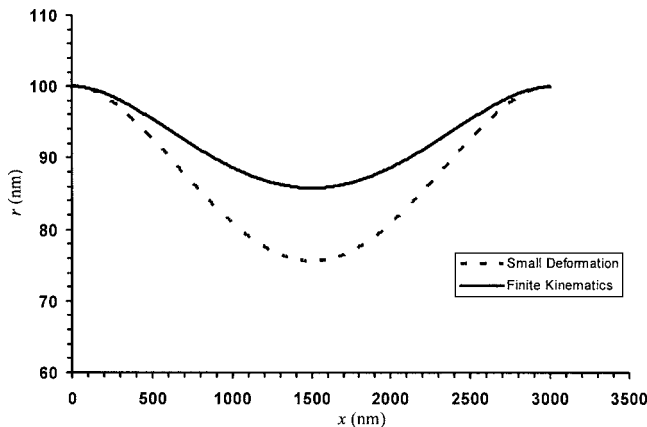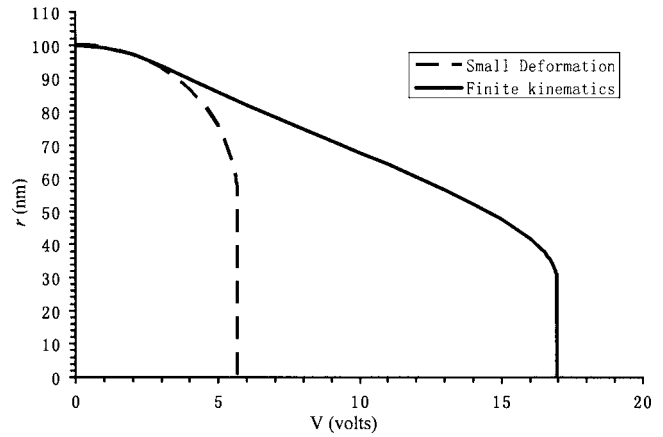
$$EI\frac{d^2}{dx^2}\left(\frac{\frac{d^2w}{dx^2}}{\left(1+\left(\frac{dw}{dx}\right)^2\right)^{3/2}}\right)$$
$$- \frac{EA}{2L}\int_0^L\left(\frac{dw}{dx}\right)^2 dx\left(\frac{\frac{d^2w}{dx^2}}{\left(1+\left(\frac{dw}{dx}\right)^2\right)^{3/2}}\right)$$
$$= (q_{vdw} + q_{elec})\sqrt{1+\left(\frac{dw}{dx}\right)^2} \qquad (8)$$

Here the electrostatic force per unit length q_{elec} is given by Eq. (3) setting $f_c = 0$, since the tip charge concentration for this boundary condition does not take place.

If $dw/dx \ll 1$, the classical equation for small displacements, Eq. (5), which neglects the stretching of the nanotube, is again recovered. In addition, for moderately finite kinematics: $(dw/dx)^2 \ll 1$, so that Eq. (8) becomes

Fig. 5 Elastic line for fixed-fixed nanotube at V=5 V. The solid line is for finite kinematics, the dotted line assumes small deformations.
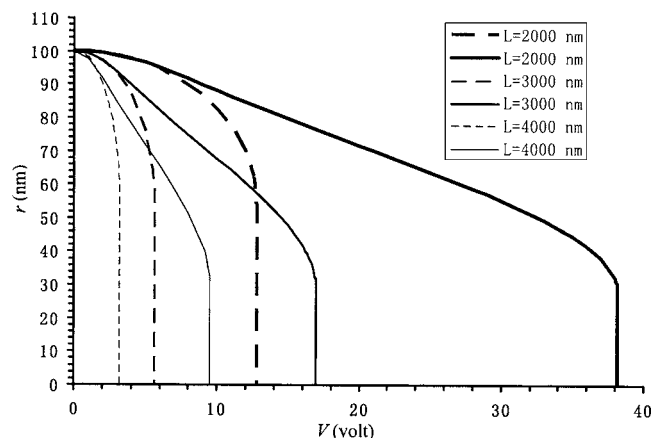

Fig. 7 Electromechanical characteristics (central displacement-voltage curve) for fixed-fixed nanotube devices with different lengths L. The dashed lines are for small deformation model (pure bending), the solid lines are for finite kinematics model (bending plus stretching).
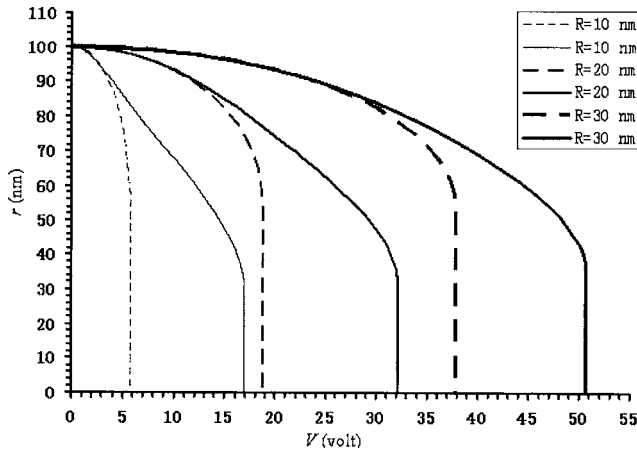
Fig. 8 Electromechanical characteristics (central displacement-voltage curve) for fixed-fixed nanotube devices with different R_{ext} and H=100 nm. The dashed lines are for small deformation model (pure bending), the solid lines are for finite kinematics model (bending plus stretching).

$$EI\frac{d^4w}{dx^4} - \frac{EA}{2L}\int_0^L\left(\frac{dw}{dx}\right)^2 dx\frac{d^2w}{dx^2} = q_{elec} + q_{vdw} \qquad (9)$$

4 Nonlinear Numerical and Theoretical Pull-In Voltage Predictions

Solving numerically the previous nonlinear equations for singly, and doubly clamped nanotube NEMS devices by direct integration (Eqs. (4) and (5)) and finite difference method (Eqs. (5) and (9)), respectively, the *pull-in* voltage corresponding to the nanotube collapsing onto the ground substrate can be predicted. This parameter is key in an optimal device design, corresponding to the transition between open and close states in applications such as nano-switches, nano-tweezers, etc.

The computed results are reported in Figs. 5–9 for doubly clamped and in Figs. 10 and 11 for singly clamped nanotube devices. Unless otherwise specified we have considered R_{ext} =10 nm, R_{int}=0, E=1 TPa, H=100 nm, and for fixed-fixed nanotube L=3000 nm, whereas for cantilever nanotube L =500 nm. In Fig. 5, the elastic lines of the nanotube under a difference in the electrostatic potential of 5 V are reported. The solid line corresponds to the finite kinematics case while the dash
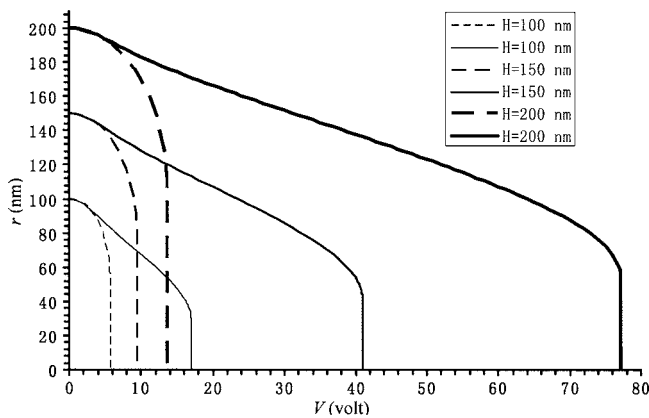

Fig. 9 Electromechanical characteristics (central displacement-voltage curve) for fixed-fixed nanotube devices with different H. The dashed lines are for small deformation model (pure bending), the solid lines are for finite kinematics model (bending plus stretching).
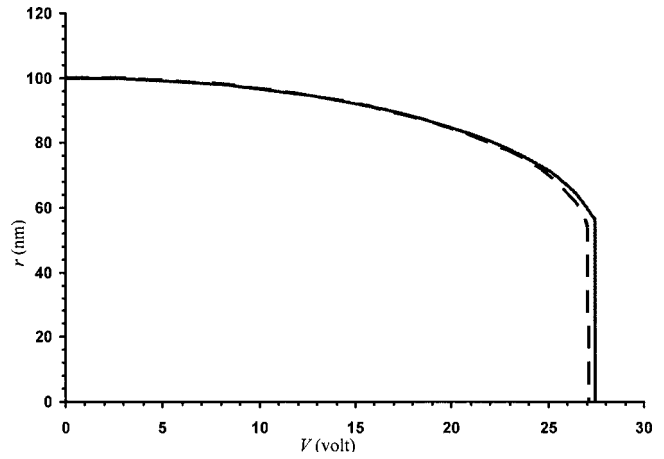

Fig. 10 The effect of finite kinematics on the characteristics of the cantilever nanotube based device (tip displacement versus voltage). The solid lines show the result accounting for finite kinematics, while the dashed line shows the result if finite kinematics is neglected. Both cases consider the concentrated charge at the end of the cantilever nanotube.

line corresponds to the small deformations case. The role of stiffening due to the rope-like behavior is quite remarkable. In Fig. 6 the central deflection of the nanotube as a function of the applied voltage is reported for both cases, i.e., with and without stretching. The two vertical lines correspond to the reaching of the pull-in voltages. In Figs. 7 and 8 similar results considering different lengths and radii are reported for both cases. Again, the role of the stretching has been found not negligible. The effect of H on the pull-in voltage is illustrated in Fig. 9. It is interesting to note that when H changes from 100 to 200 nm the pull-in voltage more than quadruples.

For the cantilevered nanotube, the displacement of the tip as a function of the applied voltage is reported in Fig. 10. In this figure, the effect of the finite kinematics is shown. As expected, the role of the finite kinematics becomes less significant than for the doubly clamped boundary condition. The pull-in voltages (instabilities) correspond to the vertical lines. Both numerical solutions reported in Fig. 10 consider the charge concentration at the tip of
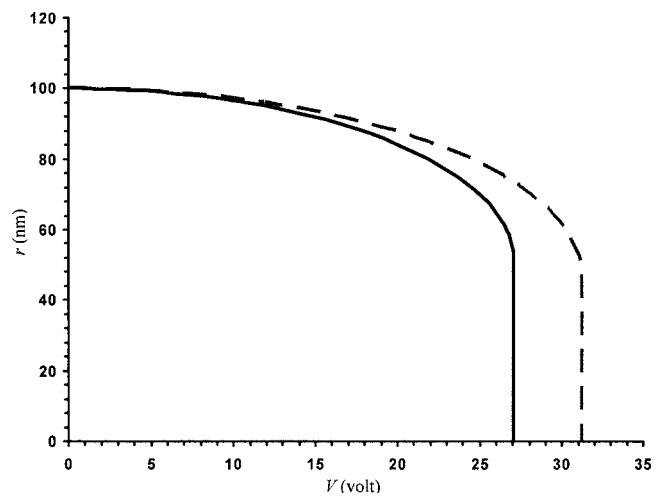

Fig. 11 The effect of the charge concentration on the characteristics of the cantilever nanotube based device (tip displacement versus voltage). The solid line shows the deflection curve with the concentrated charge. The dashed line shows the deflection curve without the concentrated charge. Both curves are from small deflection model.

Table 1 Comparison between pull-in voltages evaluated numerically and theoretically ([24,25]) by Eqs. (10) for doubly (D) and singly (C) clamped nanotube devices, respectively, E=1 TPa, R_{int}=0. For cantilever nanotube device the symbol (w) denotes that the effect of charge concentration has been included.

Case	BC	H [nm]	L [nm]	$R=R_{ext}$ [nm]	V_{PI} [V] (theo. linear)	V_{PI} [V] (num. linear)	V_{PI} [V] (theo. non-linear)	V_{PI} [V] (num. non-linear)
1	D	100	4000	10	3.20	3.18	9.06	9.54
2	D	100	3000	10	5.69	5.66	16.14	16.95
3	D	100	2000	10	12.81	12.73	36.31	38.14
4	D	150	3000	10	9.45	9.43	38.93	40.92
5	D	200	3000	10	13.53	13.52	73.50	77.09
6	D	100	3000	20	19.21	18.74	31.57	32.16
7	D	100	3000	30	38.57	37.72	51.96	50.63
8	S	100	500	10	27.28w	27.05(w)	27.52(w)	27.41 (w)
9	S	100	500	10	27.28(w)	27.05(w)	30.87	31.66

the cantilever nanotube. Figure 11 shows the error in the pull-in voltage, if the charge concentration is ignored. It is inferred that the error can be appreciable.

Recently, analytically derived formulas to compute the pull-in voltage, corresponding to the approximated solutions of the previous nonlinear equations, have been obtained equating to zero the first two derivatives (related to equilibrium and instability) of the free energy of the system [24,25]. Because devices of interest have gaps in the range of 0.1–1 μm, achievable with currently available manufacturing techniques, the effect of van der Waals force is negligible before pull-in happens [15]. Thus, we consider cases in which $q_{vdw} \approx 0$ in the analytical analysis [24] and in the comparison between numerical and analytical predictions. Accordingly, the pull-in voltages for singly (S) clamped NEMS devices can be computed as

$$V_{PI}^{S} \approx k_S \sqrt{1 + K_S^{FK}} \frac{H}{L^2} \ln\left(\frac{2H}{R_{ext}}\right) \sqrt{\frac{EI}{\varepsilon_0}}, \quad (10a)$$

$$k_S \approx 0.85, \quad K_S^{FK} \approx \frac{8H^2}{9L^2} \quad (10b)$$

Subscripts S refer to single clamped boundary conditions. Superscript FK refers to finite kinematics. Moreover, taking into account the additional energy concentrated at the tip of the cantilever nanotube and following the method described in [24], one finds the additional corrective term for the charge concentration at the tip, according to Eq. (1), as

$$V_{PI}^{S\,TIP} = \frac{V_{PI}^S}{\sqrt{1 + K^{TIP}}}, \quad K^{TIP} \approx \frac{2.55[R_{ext}(H + R_{ext})^2]^{1/3}}{L} \quad (10c)$$

For doubly (D) clamped NEMS devices, the pull-in voltage can be expressed as

$$V_{PI}^{D} = k_D \sqrt{1 + k_D^{FK}} \frac{H+R}{L^2} \ln\left(\frac{2(H+R)}{R}\right) \sqrt{\frac{EI}{\varepsilon_0}} \quad (11a)$$

$$k_D = \sqrt{\frac{1024}{5\pi S'(c_{PI})}\left(\frac{c_{PI}}{H+R}\right)}, \quad k_D^{FK} = \frac{128}{3003}\left(\frac{c_{PI}}{\rho}\right)^2 \quad (11b)$$

$$\rho^2 = \frac{I}{A} = \frac{R_{ext}^2 + R_{int}^2}{4}$$

$$S(c) = \sum_{i=1}^{\infty}\left(\frac{1}{\left[\ln\left(\frac{2(H+R)}{R}\right)\right]^i}\sum_{j=1}^{\infty} a_{ij}\left(\frac{c}{(H+R)}\right)^j\right) \quad (11c)$$

Subscripts D refer to double clamped boundary conditions; c_{PI} is the central deflection of the nanotube at the pull-in, and the $\{a_{ij}\}$ in Eq. (11c) are known constants [25].

From the Figs. 6–10 numerically predicted pull-in voltages can be obtained. We compare these results with the theoretical predictions resulting from Eqs. (10) and (11). Note that the comparison does not involve a best fit parameter. The results are reported in Table 1. Columns six and seven in Table 1 compare analytical and numerical pull-in voltage predictions under the assumption of small deformations. The agreement is good (with a maximum discrepancy of 5%). Columns eight and nine in Table 1 compare analytical and numerical pull-in voltage predictions under the assumption of finite kinematics.

5 Conclusions

In this paper a nonlinear analysis for singly and doubly clamped nanotube based nano-electromechanical system (NEMS) devices has been reported. Assuming Continuum Mechanics, the complete nonlinear equation of the elastic line of the nanotube is first derived and then numerically solved for the two considered boundary conditions. The analysis emphasizes the important role of the nonlinear effects in the prediction of the pull-in voltage, a key design parameter corresponding to the switching between the on/off states of the device. Moreover, the nonlinear analysis, neglected in previous studies, shows that finite kinematics resulting in stretching, significantly influences the pull-in voltage of doubly clamped devices. In the case of singly clamped nanotube devices, the finite kinematics effect is negligible but the effect of charge concentration is quite significant. The numerical results agree with the theoretical predictions, Eqs. (10) and (11), for the case of singly and doubly clamped nanotubes. A correction is required to account for tip charge concentration, as described by Eq. (10c). In summary, Eqs. (10) and (11) can be used with confidence in the design of novel NEMS. Moreover, these formulas can be employed to gain insight into the effect of device geometry and architecture.

References

[1] Yang, Y. T., Ekinci, K. L., Huang, X. M. H., Schiavone, L. M., Roukes, M. L., Zorman, C. A., and Mehregany, M., 2001, "Monocrystalline Silicon Carbide Nanoelectromechanical Systems," Appl. Phys. Lett., **78**, pp. 162–164.

[2] Cleland, A. N., and Roukes, M. L., 1996, "Fabrication of High Frequency Nanometer Scale Mechanical Resonators from Bulk Si Crystals," Appl. Phys. Lett., **69**, pp. 2653–2655.

[3] Erbe, A., Blick, R. H., Tilke, A., Kriele, A., and Kotthaus, P., 1998, "A Mechanical Flexible Tunneling Contact Operating at Radio Frequency," Appl. Phys. Lett., **73**, pp. 3751–3753.

[4] Huang, X. M. H., Zorman, C. A., Mehregany, M., and Roukes, M. L., 2003, "Nanodevice Motion at Microwave Frequencies," Nature (London), **421**, p. 496.

[5] Roukes, M. L., 2000, "Nanoelectromechanical System," Technical Digest of the 2000 Solid-State Sensor and Actuator Workshop.

[6] Abadal, G., Davis, Z. J., Helbo, B., Borrise, X., Ruiz, R., Boisen, A., Campabadal, F., Esteve, J., Figueras, E., Perez-Murano, F., and Barniol, N., 2001, "Electromechanical Model of a Resonating Nano-Cantilever-Based Sensor for High-Resolution and High-Sensitivity Mass Detection," Nanotechnology, **12**, pp. 100–104.

[7] Martel, R., Schmidt, T., Shea, H. R., Hertel, T., and Avouris, Ph., 1998, "Single- and Multi-Wall Carbon Nanotube Field-Effect Transistors," Appl. Phys. Lett., **73**, pp. 2447–2449.

[8] Cleland, A. N., and Roukes, M. L., 1998, "A Nanometer-Scale Mechanical Electrometer," Nature (London), **392**, pp. 160–162.

[9] Akita, S., Nakayama, Y., Mizooka, S., Takano, Y., Okawa, T., Miyatake, Y., Yamanaka, S., Tsuji, M., and Nosaka, T., 2001, "Nanotweezers Consisting of Carbon Nanotubes Operating in an Atomic Force Microscope," Appl. Phys. Lett., **79**, pp. 1691–1693.

[10] Kim, P., and Lieber, C. M., 1999, "Nanotube Nanotweezers," Science, **126**, pp. 2148–2150.

[11] Rueckes, T., Kim, K., Joslevich, E., Tseng, G. Y., Cheung, C., and Lieber, C. M., 2000, "Carbon Nanotube-Based Nonvolatile Random Access Memory for Molecular Computing," Science, **289**, pp. 94–97.

[12] Kinaret, J., Nord, T., and Viefers, S., 2003, "A Carbon-Nanotube-Based Nanorelay," Appl. Phys. Lett. **82**, pp. 1287–1289.

[13] Fennlmore, A. M., Yuzvlnsky, T. D., Han, W. Q., Fuhrer, M. S., Cummings, J., and Zettl, A., 2003, "Rotational Actuator Based on Carbon Nanotubes," Nature (London), **424**, pp. 408–410.

[14] Ke, C.-H., and Espinosa, H. D., 2004, "Feedback Controlled Nanocantilever Device," Appl. Phys. Lett. **85**, pp. 681–683.

[15] Dequesnes, M., Rotkin, S. V., and Aluru, N. R. 2002, "Calculation of Pull-in Voltage for Carbon-Nanotube-Based Nanoelectromechanical Switches," Nanotechnology, **13**, pp. 120–131.

[16] Krcmar, M., Saslow, W. M., and Zangwill, A., 2003, "Electrostatic of Conducting Nanocylinder," J. Appl. Phys., **93**, pp. 3495–3500.

[17] Hayt, W., and Buck, J., 2001, *Engineering Electromagnetics*, 6th ed., McGraw–Hill, New York.

[18] Keblinski, P., Nayak, S. K., Zapol, P., and Ajayan, P. M., 2002, "Charge Distribution and Stability of Charged Carbon Nanotube," Phys. Rev. Lett., **89**, p. 255503.

[19] Bulashevich, K. A., and Rotkin, S. V., 2002, "Nanotube Devices: A Microscopic Model," JETP Lett., **175**, pp. 205–209.

[20] Rotkin, S. V., Shrivastava, V., Bulashevich, K. A., and Aluru, N. R., 2002, "Atomic Capacitance of a Nanotube Electrostatic Device," Int. J. Nanosci., **1**, pp. 337–346.

[21] Ke, C.-H., and Espinosa, H. D., 2005, "Numerical Analysis of Nanotube Based NEMS Devices—Part I: Electrostatic Charge Distribution on Multiwalled Nanotubes," ASME J. Appl. Mech., **72**, pp. 721–725.

[22] Fertis, D. G., 1999, *Nonlinear Mechanics*, 2nd ed. CRC, Boca Raton, FL.

[23] Sathyamoorthy, M., 1998, *Nonlinear Analysis of Structures*, CRC, Boca Raton, FL.

[24] Ke, C-H., Pugno, N., Peng, B., and Espinosa, H. D., 2005, "Experiments and Modelling of Carbon-Nanotube Based NEMS Devices," J. Mech. Phys. Solids, **53**, pp. 1314–1333.

[25] Pugno, N., Ke, C.-H., and Espinosa, H. D., 2005, ″Analysis of Doubly-Clamped Nanotube Devices Under Large Displacements,″ ASME J. Appl. Mech., **72**, pp. 445–449.